Manuscript Details

Manuscript number	INOCHE_2018_505
Title	Syntheses, supramolecular architectures and photoluminescence properties of Zn(II) complexes based on 3,5-dihydroxybenzoic and pyridine/pyrazole derived ligands
Article type	Short Communication

Abstract

Five new coordination compounds [Zn(μ-3,5-DHB)2(H2O)2]n (1a), [Zn(μ-3,5-DHB)(μ-OH2)(H2O)2]n·(3,5-DHB)n·(4H2O)n (1b), [Zn(3,5-DHB)2(Isna)2]·2H2O (2), [Zn(3,5-DHB)2(4-Acpy)2]·3H2O (3) and [Zn(3,5-DHB)2(3-Mepz)2]·H2O (4) (3,5-HDHB = 3,5-dihydroxybenzoic, Isna = isonicotinamide, 4-Acpy = 4-acetylpyridine and 3-Mepz = 3-methylpyrazole) were synthesized in water or water-methanol as solvents. All these compounds have been characterized by elemental analysis, FTIR-ATR and 1H-NMR spectroscopies and Powder X-ray diffraction (PXRD). For compounds 1b-4, X-ray crystal structures have been determined. In these compounds, 3,5-DHB ligand displays different coordination modes. Complex 1b is a coordination polymer, while the addition of the pyridine/pyrazole ligands in the reaction provokes the formation of monomeric compounds (2-4). Moreover, the crystal packing indicates that these complexes expand into 2D/3D network structures mainly by intermolecular hydrogen bond interactions. Finally, the photoluminescent properties of these complexes in solid state have also been investigated. The strong emission observed for 1b indicates that it may be a good candidate for photoluminescent devices.

Keywords	Zn(II) complexes; N-heterocyclic ligands; coordination polymer; supramolecular network; photoluminescence properties.

Corresponding Author	Josefina Pons
Corresponding Author's Institution	Universitat Autònoma de Barcelona
Order of Authors	Miguel Guerrero, Roger Pou, Laura Bayés-García, Mercè Font-Bardia, Jordi Sort, Josefina Pons, Jose A. Ayllon

Submission Files Included in this PDF

File Name [File Type]

Letter_INOCHE.docx [Cover Letter]

Highlights_Def.docx [Highlights]

Graphical abstract.tif [Graphical Abstract]

Roger Inoche_resub.docx [Manuscript File]

R_Inoche_Supp-resub.docx [Supporting File]

Submission Files Not Included in this PDF

File Name [File Type]

Cristalographic information.7z [Crystallographic Data (.zip)]

To view all the submission files, including those not included in the PDF, click on the manuscript title on your EVISE Homepage, then click 'Download zip file'.

This manuscript contains content innovation file(s).
General instructions for reviewing content innovation files can be found here.

Dear Prof. Belluco,

According to the advices of your last mail, dated last 16th June (attached below), we return to send the article, which previously had reference number INOCHE_2018_331.

On this occasion, and following your guidelines, we have revised the article thoroughly, so this new version is now in line with the demands of Inorganic Chemistry Communications. Concretely, we have combined all former sections into a single untitled section that contains only the essential information, and reduced the number of figures. We have also placed experimental details and additional tables and figures in the supplementary data.

Sincerely yours

Dr. Josefina Pons

****

From: mirto.mozzon <mirto.mozzon@unipd.it>

Date: 16 de junio de 2018, 18:43:16 CEST

To: <Josefina.Pons@uab.cat>, "icaub@tin.it" <icaub@tin.it>

Subject: Fwd: Ref: INOCHE_2018_331

Dear Prof. Pons,

After reconsideration of the comments of the three Referees of your manuscript INOCHE_2018_331 I inform you that your judgments are accurate for a reassessment of your manuscript.

Please resubmit your paper as a new manuscript according to the following guidelines:

“Communications should be written in the correct format (i.e. the Introduction, Experimental, Results and Discussion sections combined into a single untitled section) and only hold essential information in no more than three printed pages. Any experimental detail that cannot be briefly described should be placed in the footnotes, the references, or stored online as supplementary data”.

Best regards.

Mirto Mozzon

ICA and INOCHE Assistant Editor

Belluco Receiving Editorial Office

Highlights

3,5-Dihydroxybenzoate of Zn(II) contains positively charged chains with both carboxylate and aqua bridges.

Addition of N-donors ligands yields monomeric complexes with tetrahedral or bipyramidal geometry.

3,5-Dihydroxybenzoate of Zn(II) shows strong blue photolumincence emission.

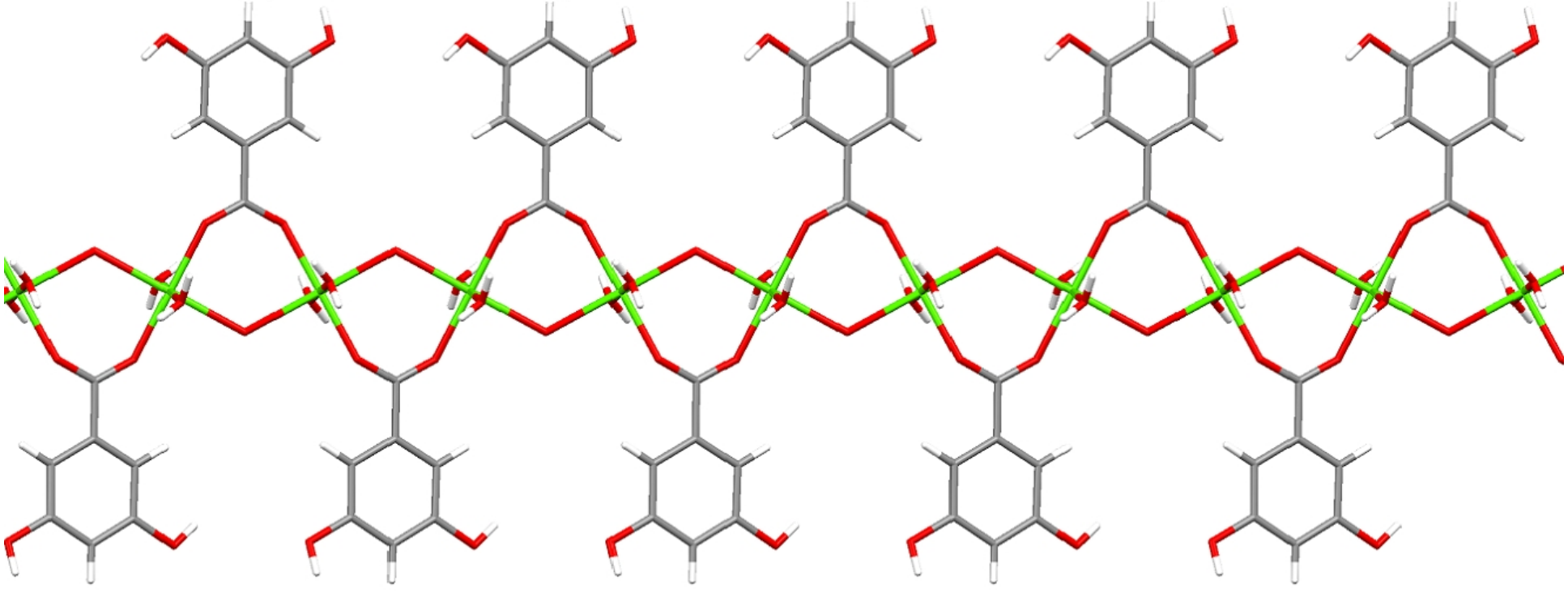

Syntheses, supramolecular architectures and photoluminescence properties of Zn(II) complexes based on 3,5-dihydroxybenzoic and pyridine/pyrazole derived ligands

Miguel Guerrero,[a,b] Roger Pou,[a] Laura Bayés-García,[c] Mercè Font-Bardia,[d] Jordi Sort,[b,e] Josefina Pons,[a,*] and José A. Ayllón,[a,*]

[a]*Departament de Química, Universitat Autònoma de Barcelona, 08193-Bellaterra, Barcelona, Spain*

[b] *Departament de Física, Universitat Autònoma de Barcelona, 08193-Bellaterra, Barcelona, Spain*

[c]*Secció de Cristal·lografia, Mineralogia i Dipòsits Minerals, Universitat de Barcelona, Martí i Franquès s/n, 08028-Barcelona, Spain.*

[d]*Unitat de Difracció de Raig-X, Centres Científics i Tecnològics de la Universitat de Barcelona (CCiTUB), Universitat de Barcelona, Solé i Sabarís, 1-3, 08028-Barcelona, Spain.*

[e]*Institució Catalana de Recerca i Estudis Avançats (ICREA) and Departament de Física, Universitat Autònoma de Barcelona, E-08193 Bellaterra, Spain.*

Keywords: Zn(II) complexes; *N*-heterocyclic ligands; coordination polymer**;** supramolecular network; photoluminescence properties.

Abstract

Five new coordination compounds $[Zn(\mu\text{-}3,5\text{-}DHB)_2(H_2O)_2]_n$ **(1a)**, $[Zn(\mu\text{-}3,5\text{-}DHB)(\mu\text{-}OH_2)(H_2O)_2]_n\cdot(3,5\text{-}DHB)_n\cdot(4H_2O)_n$ **(1b)**, $[Zn(3,5\text{-}DHB)_2(Isna)_2]\cdot 2H_2O$ **(2)**, $[Zn(3,5\text{-}DHB)_2(4\text{-}Acpy)_2]\cdot 3H_2O$ **(3)** and $[Zn(3,5\text{-}DHB)_2(3\text{-}Mepz)_2]\cdot H_2O$ **(4)** (3,5-HDHB = 3,5-dihydroxybenzoic, Isna = isonicotinamide, 4-Acpy = 4-acetylpyridine and 3-Mepz = 3-methylpyrazole) were synthesized in water or water-methanol as solvents. All these compounds have been characterized by elemental analysis, FTIR-ATR and ^{1}H-NMR spectroscopies and Powder X-ray diffraction (PXRD). For compounds **1b-4,** X-ray crystal structures have been determined. In these compounds, 3,5-DHB ligand displays different coordination modes. Complex **1b** is a coordination polymer, while the addition of the pyridine/pyrazole ligands in the reaction provokes the formation of monomeric compounds (**2-4**). Moreover, the crystal packing indicates that these complexes expand into 2D/3D network structures mainly by intermolecular hydrogen bond interactions. Finally, the photoluminescent properties of these complexes in solid state have also been investigated. The strong emission observed for **1b** indicates that it may be a good candidate for photoluminescent devices.

Supramolecular chemistry involving coordination polymers constructed from transition metal is of significant interest to the crystal engineering community since their potential applications as storage devices, catalysis, luminescent materials, magnetism or sensors, among others, have been remarkably boosted during recent years [1]. One of the key factors in the network design is the metal-ligand coordinate-covalent bond whose directionality and strength leads to the formation of different supramolecular architectures. Interestingly, the dimensionality of the resulting coordination network can be increased by adding selective non-covalent interactions (i.e. intra- and intermolecular hydrogen bondings) [2]. By a smart combination of rational-designed organic ligands with selected metal cations, a variety of novel supramolecular architectures can be obtained. For example, Zn(II) ions, with d^{10} electronic configuration, present different number of coordination and spatial arrangements, varying from tetrahedral to octahedral geometry. They can readily form compounds of different nuclearity and, combined with appropriate linkers, all kinds of architectures such as 1D, 2D, and 3D structures can be obtained [3]. Carboxylate anion, frequently used as a ligand in classical coordination chemistry due to its significant ability to form stable Zn(II) complexes, is generally also employed to build coordination polymers [4]. However, the ability to predict the supramolecular assembly and crystal packing in the solid state is still nowadays a long-standing challenge [5].

As part of our research into compounds formed by carboxylate ligands and Zn(II), and compared to Cu(II) and Cd(II) metallic centre, we have studied the coordinating properties of 3,5-benzodiaxole-5-carboxylic acid (HPip) towards $[M(MeCO_2)_2]$ (M = Cu(II), Zn(II) and Cd(II)) in the presence of different pyridine ligands. For Cu(II), monomeric and dimeric compounds were synthetized [6], while for Zn(II) and Cd(II), only dimeric compounds were obtained [7].

As an extension of our previous work, we describe in this paper the synthesis and characterization of Zn(II) complexes with 3,5-dihydroxybenzoic acid (3,5-HDHB) and pyridines or pyrazole derived ligands. Complex $[Zn(\mu\text{-}3,5\text{-}DHB)_2(H_2O)_2]_n$ (**1a**) was obtained in two steps: i) reaction between ZnO nanoparticles and 3,5-HDHB in water at 100 ºC, and later ii) evaporation of the solvent at 60 ºC overnight. When compound **1a** was recrystallized in water, $[Zn(\mu\text{-}3,5\text{-}DHB)(\mu\text{-}OH_2)(H_2O)_2]_n\cdot(3,5\text{-}DHB)_n\cdot(4H_2O)_n$ (**1b**) was obtained (Scheme 1). The compound **1b** is a coordination polymer, that contains positively charged chains compensated by non-coordinated 3,5-DHB anions (Fig. 1). The asymmetric unit consists of two zinc centers in a special position (inversion center), one bridged 3,5-DHB ligand, one bridged water, two coordinated water molecules, one uncoordinated 3,5-DHB anion and four uncoordinated water solvent molecules. Each of the independent zinc centers is six-coordinated and possesses a distorted octahedral geometry. The two zinc centers are bridged by O(10) from a water molecule and one $\mu\text{-}\kappa^1O,\kappa^1O'$-carboxylate group, from a 3,5-DHB ligand. Both bridges are roughly coplanar and define a seven atoms ring (Zn-O-C-O-Zn-O_{water}-Zn). The coordination of each Zn(II) is completed by two monodentate aqua ligands, that are perpendicular to the bridge. Polymeric Zn chains along [010] direction were connected by zig-zag arranged H-bonds along the [100] direction. Thus, each oxygen of the carboxylate group, of non-coordinated 3,5-DHB ligand is linked by hydrogen bond with (non-bridging) aqua ligand of adjacent polymeric chains in the ***a*** direction (O9-H9A···O6: 1.90 Å, 176º and O11-H11A···O5: 1.90 Å, 171º) while one of the phenol group of a coordinated 3,5-DHB anion (O3-H3A···O8: 1.86 Å, 172º), connecting adjacent chain in the ***c*** direction. Thus, a complex 3D supramolecular network is established. Non-coordinated water molecules are also hydrogen bonded (Table S5). Finally, intermolecular π-stacking interactions

with a mean distance of 3.7 Å were also determined between coordinated and non-coordinated 3,5-DHB aromatic rings (Fig. 1c).

Monomeric compounds $[Zn(3,5\text{-}DHB)_2(Isna)_2]\cdot 2H_2O$ (**2**), $[Zn(3,5\text{-}DHB)_2(4\text{-}Acpy)_2]\cdot 3H_2O$ (**3**) and $[Zn(3,5\text{-}DHB\text{-}\kappa\text{-}O)(3,5\text{-}DHB\text{-}\kappa^2\text{-}O,O)(3\text{-}Mepz)_2]\cdot H_2O$ (**4**). were prepared by reaction of compound **1a** with isonicotinamide (Isna) (**2**), 4-acetylpyridine (4-Acpy) (**3**) or 3-methylpyrazole (3-Mepz) in water/methanol solvent at room temperature (Scheme 1, Fig. 2). In **2** and **3**, the zinc ion is four-coordinated with two Zn-N bonds (*N*-Isna, *N*-4-Acpy) and two Zn-O bonds that correspond to two monodentate carboxylates from two 3,5-DHB ligands. The coordination geometry is distorted tetrahedral. The $Zn\text{-}O_{carbox}$ the Zn-N bond lengths are comparable with those previously reported $[Zn(3,5\text{-}DHB)_2(py)_2]\cdot 1.25CH_2Cl_2\cdot 0.75CH_3OH$ (py = pyridine)[8]. Interestingly in **4** one 3,5-DHB ligand acts as a bidentate chelate while the other acts as monodentate. This complex has a $[ZnO_3N_2]$ *core* ($\tau = 0.47$) [9], exhibiting a geometry between square-pyramidal and distorted trigonal-bipyramid. The equatorial plane is defined by two O (one of the monodentate (O5), other of the bidentate chelate (O1)), and one N3(3-Mepz) atom. In the axial position, the N1 (3-Mepz) and the O2 (bidentate chelate) atoms are present. The $[ZnN_2O_3]$ (O = carboxylate) *core* is present in 112 compounds described in the literature [10] but only four of these contain Npz [11]. Besides **4** presents intramolecular hydrogen bond between one nitrogen pyrazolic atom and a non-coordinated O atom of the carboxylate group (3,5-DHB ligand) complex (N2-H2···O6: 2.05 Å, 137º), yielding a seven-membered ring with boat conformation (Table S5, Fig. S1).

Regarding the extended structure of compounds **2-4,** one may state some general trends regarding. In the tree structure a key role corresponds to hydrogen bonds between phenol group and non-coordinating oxygen atom of carboxylate group of neighboring

molecules. Isonicotinamide has been frequently used to design hydrogen bonding supramolecular networks due to its high tendency to form both homomeric and heteromeric synthons [12]. However, in **2**, the strongest intermolecular interaction observed do involve the 3,5-DHB ligand instead of the Isna ligand. The non-coordinating oxygen of each carboxylate group is linked to with a phenol group of an adjacent molecule (O3-H3O···O2: 1.77 Å, 166º). The propagation of these interactions defines 2D sheets parallel to the **ac** plane (Fig. 3a). Finally, O atoms of the amide group (Isna ligand) and non-coordinated water molecules of adjacent planes (O1W-H1WB···O5: 1.95 Å, 169º) generates a truly 3D arrangement in the space. Regarding additional intermolecular interactions, π-stacking occurred along columns ([101] direction) between 3,5-DHB and isonicotinamide aromatic rings, with an interaction distance of 3.760 Å (Fig. S2).

In compound **3**, the intermolecular hydrogen bonds between non-coordinated O of and phenol groups of adjacent molecules (O4-H4···O6: 1.81 Å, 171º, O8-H8O···O2: 2.26 Å, 113º) also defines 2D sheets parallel to the **bc** plane (Fig. 3b), that are interconnected by additional H-bonds established by water molecules. Finally, in compound **4**, the intramolecular hydrogen bond is linked to the phenol group of an adjacent 3,5-DHB (O3-H3O···O6: 1.83 Å, 179º) defines dimers. A pyrazolic ring is also involved in this dimer interaction (N4-H4N···O2: 2.26 Å, 124º) (Fig. 3c). Additional hydrogen bonds between phenol groups of neighbouring molecules (O8-H8O···O4: 2.01 Å, 156º; O7-H7O···O3: 2.03 Å, 179º) defines a 3D supramolecular network, reinforced by additional hydrogen bond in which water molecules participates.

The five compounds have been characterized by elemental analysis, FTIR-ATR and ^{1}H-NMR spectroscopies and all results agree with the composition of the crystals. Besides Powder X-ray diffraction (Fig. S3-S6) confirmed that single crystals and the bulk

samples have the same structure. Recently, luminescent compounds, especially those with d^{10} metals, have been the focus of intense interest as they have potential in a variety of applications, including photochemistry or sensors [13]. However, there is few data available on the synthesis and luminescence of these compounds. In order to clarify the structural modification effects of the ligands on Zn(II) complexes, we have performed photoluminescence studies. Therefore, the emission spectra of complexes **1**-**4** were measured in the solid state at room temperature (Fig. 4a). When compared, the photoluminescence intensities of polymeric coordination compounds 1a and 1b are larger than the ones of the monomeric compounds. This phenomenon is probably explained by the rigidity enhancement of coordinated ligands in the complexes [14]. Also, their emission peaks could be explained by the combination of the characteristics of intraligand and ligand-to-ligand charge transitions (LLCT), as Zn(II) ion belongs to d^{10} electronic configurations and is difficult to oxidize/ reduce [15]. Remarkably, contrary to fluorescent semiconductor nanocrystals, where an undesired decrease in the photoluminescence intensity is normally observed (photobleaching), here only a decrease of 5% (**1b**) – 35% (**3**) of photoluminescence intensity was obtained after irradiation during 10 min (Fig. S6b). Therefore, due to the photostability of **1b** in the photoluminescence signal and the relatively large width of the observed photoluminescence peak, this novel Zn compounds could be appealing for optoelectronic devices.

Acknowledgements

This work was financed by the Spanish National Plan of Research MAT2015-65756-R and CTQ2017-83632 by 2014SGR1015 project from the Generalitat de Catalunya.

Appendix A. Supplementary data

CCDC 1578831-1578834 contains the supplementary crystallographic data for compounds **1b-4**. The data can be obtained free of charge via http://www.ccdc.cam.ac.uk/conts/retrieving.html, or from the Cambridge Crystallographic Data Centre, 12 Union Road, Cambridge CB2 1EZ, UK; fax:(+44) 1223–336-033; or e-mail: deposit@ ccdc.cam.ac.uk.

Detailed experimental procedures, PXRD patterns and additional figures are available as electronic supplementary information in the online version can be found online at https://doi.org/10.1016/xxxxx

References

[1] (a) Z. Liu, S. K. Mo. Nalluri, J. F. Stoddart, Chem. Soc. Rev. 46 (2017) 2459-2478; (b) K. Biradha, M. Sarkar, L. Rajput, Chem. Commun. (2006) 4169–4179; (c) Y. Rachuri, B. Parmar, K. K. Bisht, E. Suresh, Dalton Trans. 46 (2017) 3623–3630.

[2] (a) T. R. Cook, Y.-R. Zheng, P. J. Stang, Chem Rev. 9 (2013) 734–777. (b) M. Guerrero, J. Pons, M. Font-Bardia, T. Calvet, J. Ros, Polyhedron 29 (2010) 1083–1087.

[3] K. Liu, W. Shi, P. Cheng, Dalton Trans. 40 (2011) 8475-8490.

[4] (a) D. A. Dickie, M. C. Jennings, H. A. Jenkins, J. A. C. Clyburne, Inorg. Chem. 44 (2005) 828–830. (b) F.-M. Jian, S.-D. Zhu, S. Jin, Z.-G. Zhou, Y.-B. Lu, Inorg. Chem. Commun. 36 (2013) 155–158. (c) Q. Meng, L. Wang, D. Wang, J. Yang, C. Yue, J. Lu, Crystals **7** (2017) 1-7.

[5] I. H. Hwang, H.-Y. Kim, M. M. Lee, Y. J. Na, J. H. Kim, H.-C. Kim, C. Kim, S. Huh, Y. Kim, S.-J. Kim, Cryst. Growth Des. 13 (2013) 4815−4823.

[6] (a) J. Soldevila-Sanmartín, J. A. Ayllón, T. Calvet, M. Font-Bardía, C. Domingo, J. Pons, Inorg. Chem. Commun. 71 (2016) 90-93; (b) J. Soldevila-Sanmartín, J. A. Ayllón, T. Calvet, M. Font-Bardía, J. Pons, Polyhedron 126 (2017) 184-194.

[7] M. Guerrero, S. Vázquez, J. A. Ayllón, T. Calvet, M. Font-Bardía, J. Pons, ChemistrySelect 2 (2017) 632-639;

[8] L. Feng, Z. Chen, M. Zeller, R. L. Luck, Inorg. Chim. Acta 394 (2013) 729-740.

[9] A. W. Addison, T. N. Rao, J. Chem. Soc., Dalton Trans. (1984) 1349-1356.

[10] F. A. Allen, Acta Crystallogr. B58 (2002) 380-388.

[11] (a) C. Obuah, Y. Lochee, J. H. L. Jordaan, D. P. Otto, T. Nyokong, Polyhedron 90 (2015) 154-164; (b) S. O. Ojwach, T. T. Okemwa, N. W. Attandoh, B. Omondi, Dalton Trans. 42 (2013) 10735-10745; (c) T. Basu, H. A. Sparkes, M. K. Bhunia, R. Mondal, Crystal Grouth Design. 9 (2009) 3488-3496. (d) J. Hunger, H. Krautscheid, J. Sieler, Cryst. Growth Des. 9 (2009) 4613-4625.

[12] (a) A. M. Beatty, Coord. Chem. Rev. 246 (2003) 131-143; (b) A. M. Beatty, CrystEngComm. 51 (2001) 1-13.

[13] (a) V. W.-W. Yam, V. K-M. Au, S. Y.-L. Leung, Chem. Rev. 115 (2015) 7589–7728; (b) M. Guerrero, J. Pons, M. Font-Bardia, T. Calvet, J. Ros, Aust. J. Chem. 63 (2010) 958–964.

[14] R.-P. Ye, X. Zhang, J.-Q. Zhai, Y.-Y. Qin, L. Zhang, Y.-G. Yao, J. Zhang, CrystEngComm. 17 (2015) 9155-9166.

[15] M. D. Allendorf, C. A. Bauer, R. K. Bhaktaa, R. J. T. Houka, Chem. Soc. Rev. 38 (2009) 1330–1332.

Scheme 1. Synthesis routes to each compound. For compound **1a** only the 1D polymeric framework is shown.

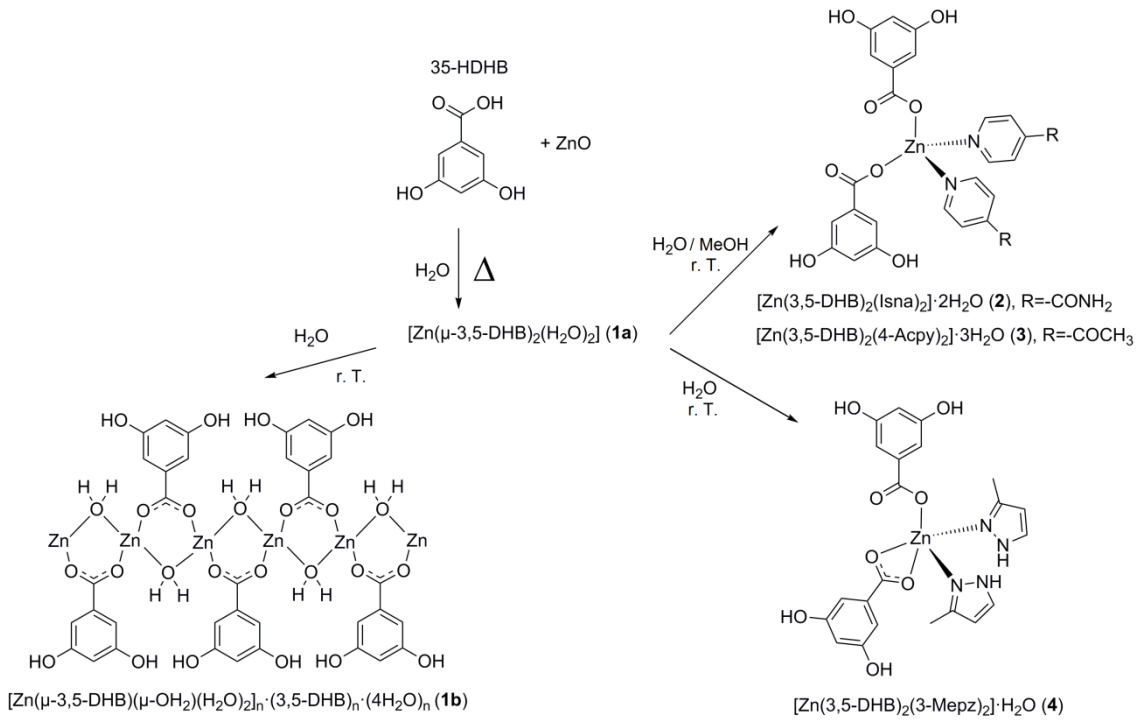

Figure captions

Figure 1. a) Crystal structure of complex $[Zn(\mu\text{-}3,5\text{-}DHB)(\mu\text{-}OH_2)(H_2O)_2]_n \cdot (3,5\text{-}DHB)_n(4H_2O)_n$ (**1b**) and b) its one-dimensional polymeric view. c) Detail showing H-bond interactions and π-stacking. Water molecules are not shown for clarity.

Figure 2. Crystal structure of complexes a) $[Zn(3,5\text{-}DHB)_2(Isna)_2]\cdot 2H_2O$ (**2**), b) $[Zn(3,5\text{-}DHB)_2(4\text{-}Acpy)_2]\cdot 3H_2O$ (**3**) and c) $[Zn(\mu\text{-}3,5\text{-}DHB)_2(3\text{-}Mepz)_2]\cdot H_2O$ (**4**), showing all non-hydrogen atoms. Water molecules are not shown for clarity.

Figure 3. Transversal view of the supramolecular 2D network in a) $[Zn(3,5\text{-}DHB)_2(Isna)_2]\cdot 2H_2O$ (**2**) and b) $[Zn(3,5\text{-}DHB)_2(4\text{-}Acpy)_2]\cdot 3H_2O$ (**3**). c) Dimer defined by intermolecular hydrogen bonds in $[Zn(\mu\text{-}3,5\text{-}DHB)_2(3\text{-}Mepz)_2]\cdot H_2O$ (**4**). Water molecules are not shown for clarity.

Figure 4 a) Spectral profiles representing photoluminescence intensity versus emission wavelength in the 400–750 nm range all described complexes. b) Photostability of the Zn(II) complex upon irradiation at its excitation wavelength (410 nm).

Figure 1

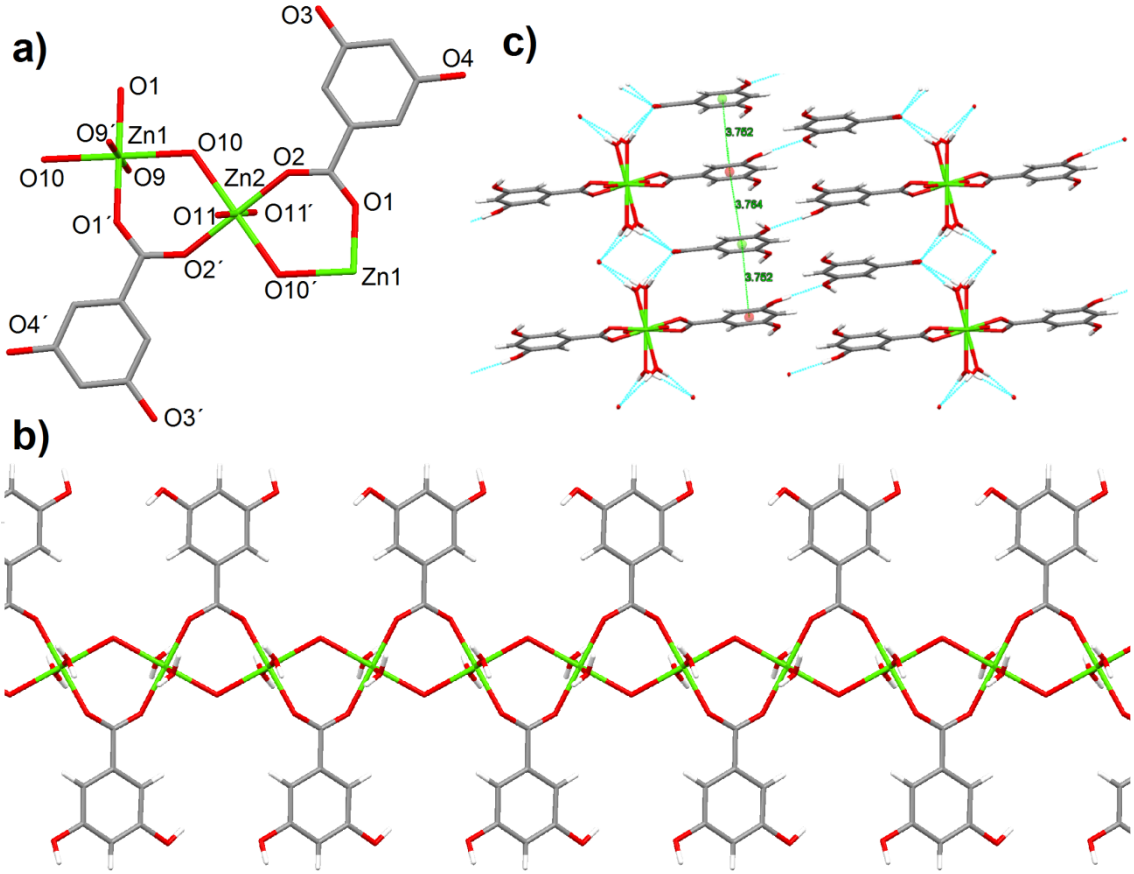
a)
O3
O4
O1
O9´
Zn1
O10
O2
O10
O9
Zn2
O1
O1´
O11
O11´
O2´
O10´
Zn1
O4´
O3´
c)
3.762
3.784
3.762
b)

Figure 2.

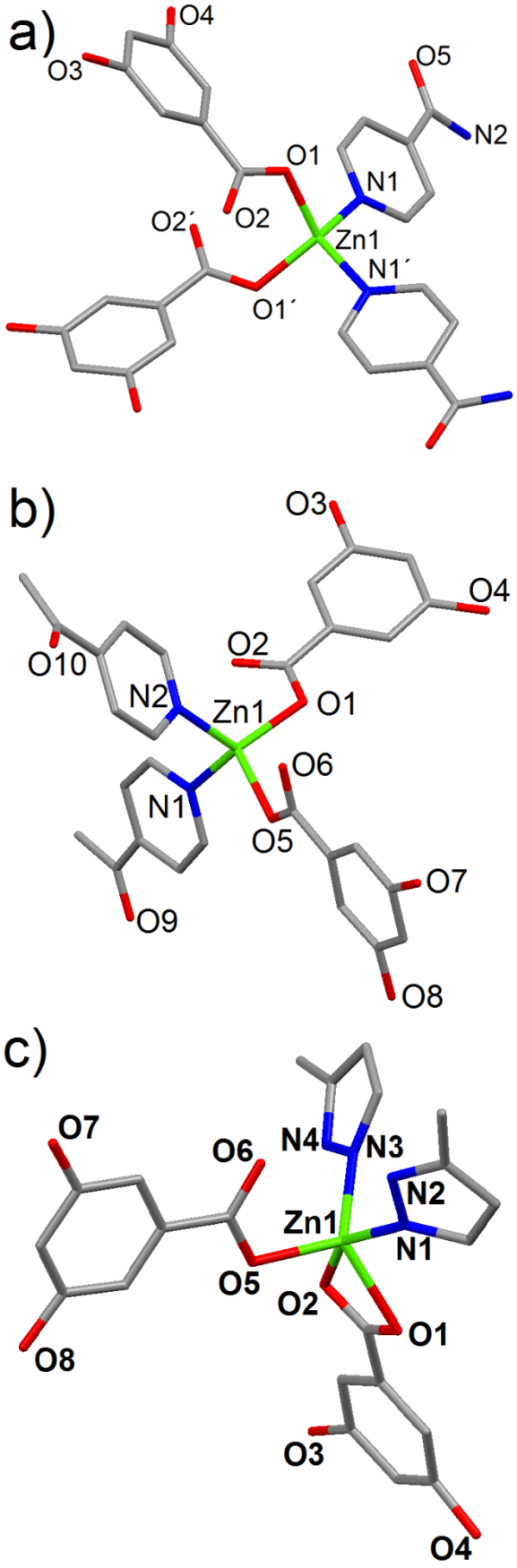
a)
O4
O3
O5
N2
O1
N1
O2´
O2
Zn1
N1´
O1´
b)
O3
O4
O10
O2
N2
Zn1
O1
O6
N1
O5
O7
O9
O8
c)
O7
O6
N4
N3
N2
Zn1
N1
O5
O2
O1
O8
O3
O4

Figure 3.

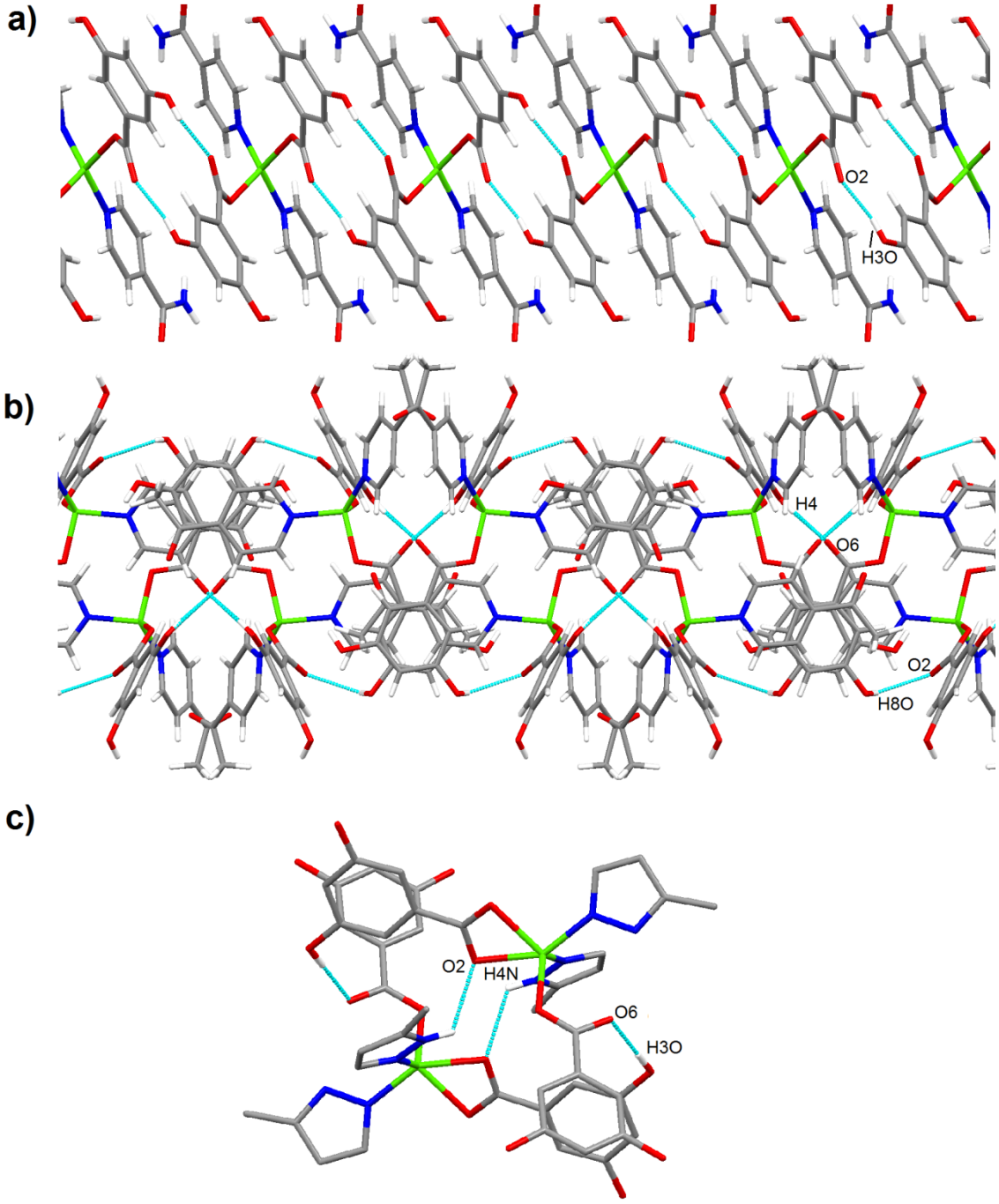

Figure 4

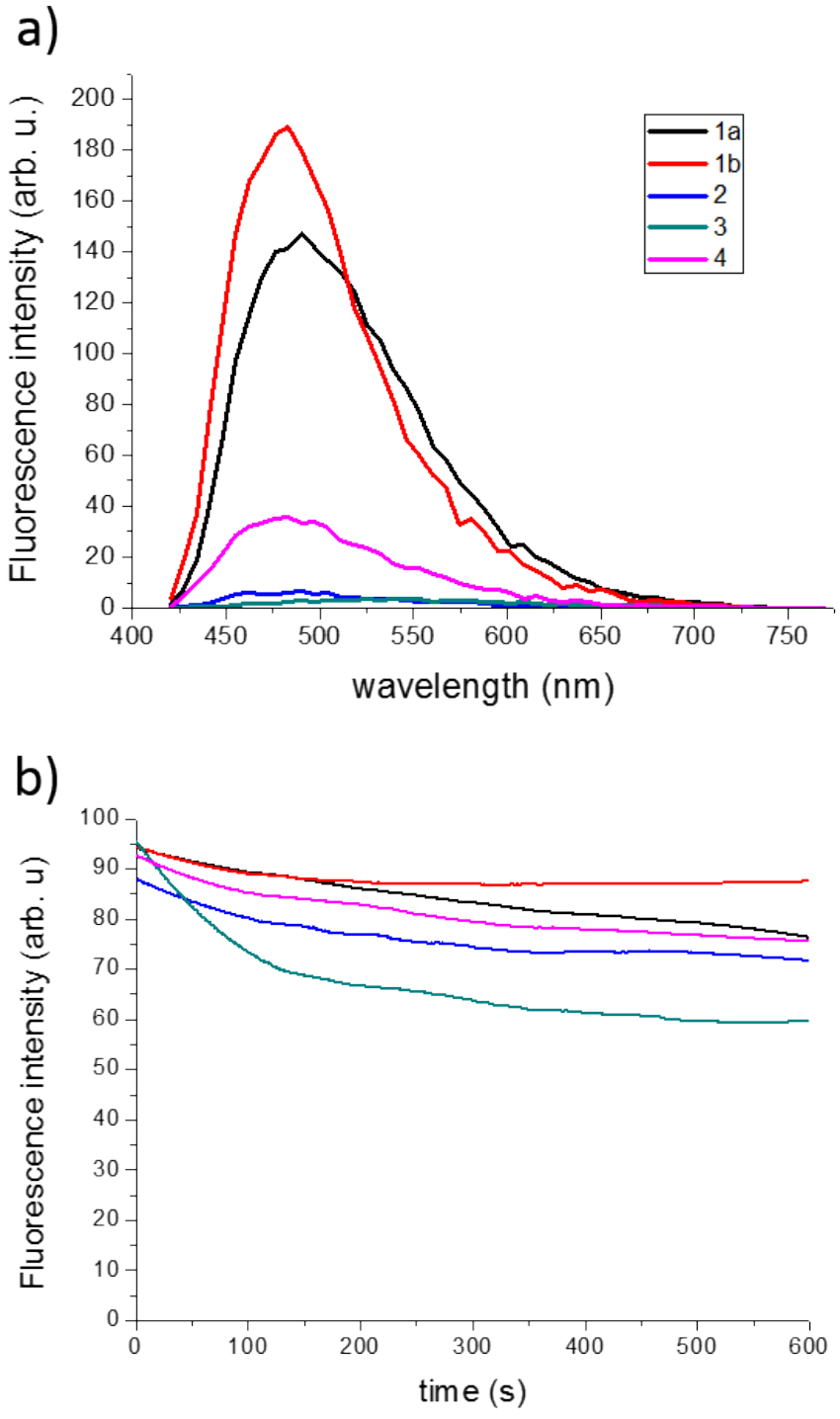
a)
Fluorescence intensity (arb. u.)
wavelength (nm)
1a
1b
2
3
4
b)
Fluorescence intensity (arb. u)
time (s)

Supplementary data

Syntheses, supramolecular architectures and photoluminescence properties of Zn(II) complexes based on 3,5-dihydroxybenzoic and pyridine/pyrazole derived ligands

Miguel Guerrero,[a,b] Roger Pou,[a] Laura Bayés-García,[c] Mercè Font-Bardia,[d] Jordi Sort,[b,e] Josefina Pons,[a,*] and José A. Ayllón,[a,*]

Experimental details

1. Materials and characterization techniques

Zinc oxide nanopowder (<100 nm particle size), 3,5-dihydroxybenzoic acid (3,5-HDHB), Isonicotinamide (Isna), 4-acetylpyridine (4-Acpy) and 3-methylpyrazole (3-Mepz) ligands and methanol (MeOH) as a solvent, were purchased from Sigma-Aldrich and used without further purification. All reactions and manipulations were carried out in air. The synthesis of compound **1a** was performed at 100 ºC with evaporation in an oven at 60 ºC overnight; the other compounds were synthesized at room temperature. Elemental analyses (C, H, N) were carried out by the staff of Chemical Analysis Service of the Universitat Autònoma de Barcelona on a Euro Vector 3100 instrument. FTIR-ATR spectra were recorded at the Chemical Analysis Service of the Universitat Autònoma de Barcelona on a Tensor 27 (Bruker) spectrometer, equipped with an attenuated total reflectance (ATR) accessory model MKII Golden Gate with a diamond window in the range 4000-600 cm^{-1}. ^{1}H NMR spectra were recorded on an NMR-FT Bruker 250 MHz spectrometer in DMSO-d_6 solution at room temperature. All chemical shifts (δ) are given in ppm. The photoluminescence properties of Zn(II) complexes were studied by confocal scanning laser microscopy (CSLM). 20 mg of each complex were mounted on Ibidi culture dishes (Ibidi GmbH, Martinsried, Germany) and were

excited with a blue diode laser (410 nm) and the fluorescence intensity was recorded generating a lambda stack with emission wavelength ranging from 400 to 750 nm. Photostability studies were performed to evaluate time-lapse experiments. **1-4** complexes were photo-bleached at a full laser power of 50 mW of blue diode 410 nm. Confocal time series were recorded with intervals of 1 frame/850 ms for a period of 10 min. Data from all studies were analyzed using the LAS AF software 2.4.1 (Leica Microsystems) obtaining the variation of the normalized fluorescence values as a function of irradiation time.

2. Synthesis and ^{1}H-NMR data

*2.1. $[Zn(\mu\text{-}3,5\text{-}DHB)_2(H_2O)_2]_n$ (**1a**) and $[Zn(\mu\text{-}3,5\text{-}DHB)(\mu\text{-}OH_2)(H_2O)_2]_n\cdot(3,5\text{-}DHB)_n\cdot(4H_2O)_n$ (**1b**)*

ZnO nanoparticles (268 mg, 3.28 mmol) were added to a solution containing 3,5-dihydroxybenzoic acid (3,5-HDHB) (978 mg, 6.35 mmol) in water (20 mL). The reaction mixture was heated to 100 ºC, since all the reactive was dissolved forming a slightly yellow solution (around 5 min). Then, the solution was allowed to cool, filtered and the solvent was evaporated at 60 ºC overnight. Compound **1a** was obtained as the solid residue and it was recrystallized from water, so that crystals suitable for X-ray analysis were obtained. Crystals were filtered and washed with cold water (5 mL) and dried in air (**1b**).

1a. Yield: 1270 mg (98.0%) (with respect to 3,5-HDHB). Elemental Analyses: Calc for $C_{14}H_{14}O_{10}Zn$ (407.66): C 41.25; H 3.46. Found: C 41.02; H 3.50%. ^{1}H NMR (250 MHz; DMSO-d_6; 298 K): δ = 6.27 [2H, t, ^{4}J = 2.2 Hz, *p*-C*H*], 6.82 [4H, d, ^{4}J = 2.3 Hz, *o*-C*H*], 9.25 [4H, s, Ar-O*H*].

1b. Yield: 1280 mg (98.0%) (with respect to compound **1a**). Although the stoichiometry of this compound has been definitively established after resolution of their crystal structure from single crystal XRD data, this compound losses solvent molecules after being removed from the solution. For this reason, we found that the manipulation required to prepare the sample for EA

unavoidably leads to the loss of a water molecule for zinc atom. Elemental Analyses: Calc for $C_{14}H_{22}O_{14}Zn$ (479.70): C 35.05; H 4.62. Found: C 34.79; H 4.23%.

*2.2.[Zn(3,5-DHB)$_2$(Isna)$_2$]·2H$_2$O (**2**)*

A solution containing isonicotinamide (Isna) (155 mg, 1.27 mmol) in water (15 mL) was added to a solution of compound **1a** (253 mg, 0.620 mmol) in water (20 mL) at room temperature. The resulting yellow solution was allowed to concentrate at room temperature until a colourless crystalline precipitate was deposited. Crystals were filtered and washed with cold water (5 mL) and dried in the air. Crystals suitable for X-ray analysis were obtained. Yield: 204 mg (50.4%) (with respect to compound **1a**). Elemental Analyses: Calc for $C_{26}H_{26}N_4O_{12}Zn$ (651.88): C 47.90; H 4.02; N 8.59. Found: C 48.06; H 4.02; N 8.67%. ^{1}H NMR (250 MHz; DMSO-d_6; 298 K): δ = 6.29 [2H, t, ^4J = 2.2 Hz, *p*-C*H*], 6.84 [4H, d, ^4J = 2.2 Hz, *o*-C*H 35DHB*], 7.72 [2H, s, NH_2], 7.78 [4H, br, HC-C*H*-C-C(O)NH_2], 8.24 [2H, br, NH_2], 8.73 [4H, br, *H*C-N-C*H*], 9.25 [4H, s, Ar-O*H*].

*2.3. [Zn(3,5-DHB)$_2$(4-Acpy)$_2$]·3H$_2$O (**3**)*

A solution containing 4-acetylpyridine (4-Acpy) (150 mg, 1.24 mmol) in water:methanol (7:3) (20 mL) was added dropwise to a solution of compound **1a** (250 mg, 0.61 mmol) in water:methanol (7:3) (20 mL) at room temperature. The resulting yellow solution was concentrated at room temperature until some colourless crystals appeared out of solution. Crystals were filtered and washed with cold water (5 mL) and dried in the air. Among them, crystals suitable for X-ray analysis were obtained.

3. Yield: 326 mg (81.8%) (with respect to compound **1a**). Although the stoichiometry of this compound has been definitively established after resolution of their crystal structure from single crystal XRD data, this compound losses solvent molecules after being removed from the solution. For this reason, we found that the manipulation required to prepare the sample for EA unavoidably leads to the loss of a water molecule for zinc atom. Elemental Analyses: Calc for

$C_{28}H_{28}N_2O_{12}Zn$ (649.90): C 51.75; H 4.34; N 4.31. Found: C 51.75; H 4.12; N 4.31%. ^{1}H NMR (250 MHz; DMSO-d_6; 298 K): δ = 2.62 [6H,s, CH_3], 6.29 [2H, t, ^4J = 2.3 Hz, HO-C*H*-OH], 6.83 [4H, d, ^4J = 2.3 Hz, *H*C-C-CO_2-C*H*], 7.82 [4H, dd, ^3J = 4.4 Hz, ^4J = 1.7 Hz, HC-C*H*-C-C(O)CH_3], 8.81 [4H, dd, ^3J = 4.4 Hz, ^4J = 1.7 Hz, *H*C-N-C*H*], 9.25 [4H, s, O*H*].

*2.4. [Zn(3,5-DHB)$_2$(3-Mepz)$_2$]·H_2O (**4**)*

A solution containing 3-methylpyrazole (3-Mepz) (205 mg, 2.50 mmol) in water (15 mL) was added dropwise to a solution of compound **1a** (500 mg, 1.23 mmol) in water (20 mL) at room temperature with vigorous stirring for 30 min. The resulting yellow solution was concentrated at room temperature until some colourless crystals appeared out of solution. The obtained crystals were filtered and washed with cold water (5 mL) and dried in the air. Crystals suitable for X-ray analysis were obtained.

4. Yield: 499 mg (71.1%) (with respect to compound **1a**). Elemental Analyses: Calc for $C_{22}H_{24}N_4O_9Zn$ (553.82): C 47.71; H 4.37; N 10.12. Found: C 47.98; H 4.37; N 10.23%. ^{1}H NMR (250 MHz; DMSO-d_6; 298 K): δ = 2.20 [6H, s, CH_3], 6.00 [2H, br, HC-C*H*-C-CH_3], 6.33 [3H, br, HO-C*H*-OH], 6.84 [6H, br, *H*C-C-CO_2-C*H*], 7.45 [2H, br, HC-C*H*-NH], 9.36 [4H, s, O*H*], 12.53 [1H, s, HC-N*H*-N].

3. ATR-FTIR spectra.

[Zn(μ-3,5-DHB)$_2$(H_2O)$_2$]$_n$ (**1a***)* (wavenumber, cm^{-1}): 3312 (s) [ν(O-H)], 3188 (m) [ν(O-H)], 1680 (w), 1614 (w), 1535 (s) [ν_{as}(COO)], 1446 (w), 1421 (m), 1357 (s) [ν_s(COO)], 1247 (w), 1204 (w), 1164 (w), 1134 (s), 996 (s), 961 (w), 888 (w), 857 (w), 841 (w), 779 (s), 659 (m).

[Zn(μ-3,5-DHB)(μ-OH_2)(H_2O)$_2$]$_n$·(3,5-DHB)$_n$·(4H_2O)$_n$ (**1b**) ATR-FTIR (wavenumber, cm^{-1}): 3313 (m) [ν(O-H)], 3190 (s) [ν(O-H)], 1612 (w), 1532 (s) [ν_{as}(COO)], 1446 (w), 1418 (m), 1357 (s) [ν_s(COO)], 1300 (w), 1248 (w), 1203 (w), 1162 (w), 1135 (s), 997 (s), 959 (w), 858 (w), 840 (w), 779 (s), 660 (m).

$[Zn(3,5\text{-}DHB)_2(Isna)_2]\cdot 2H_2O$ **(2).** (wavenumber, cm^{-1}): 3404 (m) [ν(O-H)], 3201 (w) [$\nu(N\text{-}H)_{Inca}$], 3088 (m), 2897 (w) [$\nu(N\text{-}H)_{Isna}$], 2679 (m), 1676 (s) [$\nu(CO)_{Isna}$], 1581 (s) [$\nu_{as}(COO)$], 1547 (m), 1451 (s), 1422 (w), 1379 (s) [$\nu_s(COO)$], 1302 (w), 1224 (w), 1154 (s), 1064 (w), 1031 (w), 1004 (m), 953 (w), 887 (w), 850 (m), 786 (m), 757 (s), 722 (w), 682 (w), 636 (m).

$[Zn(3,5\text{-}DHB)_2(4\text{-}Acpy)_2]\cdot 3H_2O$ **(3)** (wavenumber, cm^{-1}): 3063 (br) [ν(O-H)], 1689 (s) [$\nu(CO)_{4\text{-}Acpy}$], 1545 (s) [$\nu_{as}(COO)$], 1448 (m), 1390 (s) [$\nu_s(COO)$], 1360 (s), 1321 (w), 1260 (m), 1231 (w), 1152 (s), 1060 (w), 1029 (m), 1003 (m), 968 (w), 877 (w), 858 (w), 830 (m), 784 (s), 679 (m).

$[Zn(3,5\text{-}DHB)_2(3\text{-}Mepz)_2]\cdot H_2O$ **(4)** (wavenumber, cm^{-1}): 3287 (br) [ν(O-H)], 3090 (w), 1533 (s) [$\nu_{as}(COO)$], 1452 (m), 1407 (s), 1368 (s) [$\nu_s(COO)$], 1317 (s) [$\nu_s(COO)$], 1291 (m), 1247 (w), 1150 (s), 1126 (m), 1113 (w), 1016 (w), 1001 (m), 959 (m), 891 (w), 863 (w), 768 (s), 671 (m), 658 (m).

FTIR-ATR spectra of all compounds confirm the presence of 3,5-DHB ligand, besides for compounds **2-4**, the bands attributable to pyridines and pyrazole ligands (Isna, 4-Acpy and 3-Mepz) are observed. All IR spectra displayed the characteristic carboxylate bands in the range 1581-1532 cm^{-1} for $\nu_{as}(CO_2)$ and at 1390-1357 cm^{-1} for $\nu_s(CO_2)$ and were fully consistent with their formulations (SI, Figure S5-S9). For **1a** and **1b**, the differences between $\nu_{as}(CO_2)$ and $\nu_s(CO_2)$ are 178 and 175 cm^{-1} respectively, indicating that in both compounds the carboxylates show a bidentate bridging coordination mode. For compounds **2-4**, the differences are 202, 195 and 216 cm^{-1} respectively, indicating the presence of monodentate carboxylate ligands in these compounds. Moreover, for compound **4** other Δ value of $\nu_{as}(CO_2)$ and $\nu_s(CO_2)$ is observed, 165 cm^{-1}, indicating the presence of bidentate chelate carboxylate group [1]. The absence of a band at 1720-1690 cm^{-1} in the five compounds indicates that the carboxylic acid is deprotonated in the corresponding compounds. The bands attributable to the aromatic groups $\nu(C{=}C)_{ar}$, $\nu(C{=}N)_{ar}$, $\delta(C{=}C)_{ar}$, $\delta(C{=}N)_{ar}$, $\delta(C\text{-}H)_{ip}$ and $\delta(C\text{-}H)_{oop}$ are also observed [2].The IR spectral data thus clearly lend support to the structures determined by X-ray diffraction method.

3. X-ray crystallography

For compound **1b**, suitable crystals for X-ray analysis, a yellow needle-like specimen, were obtained from recrystallization of **1a** in water. For compounds **2-4**, crystals suitable for X-ray crystallographic analysis, colorless prism-like specimens in all cases, were grown via slow evaporation of their solutions. The X-ray data were measured on a D8 Venture system equipped with a multilayer mono-chromate and a Mo microfocus (λ = 0.71073 Å). For **1-4**, the frames were integrated with the Bruker SAINT Software package using a narrow-frame algorithm. For compound **1b**, the integration of the data using a triclinic unit cell yielded a total of 22880 reflections to a maximum θ angle of 27.15º (0.78 Å resolution), of which 4174 were independent (average redundancy 5.482, completeness = 99.8%), (Rint = 3.21%, Rsig = 2.20%) and 3557 (85.22%) were greater than $2\sigma(F^2)$. The calculated minimum and maximum transmission coefficients (based on crystal size) were 0.6583 and 0.7455. For compound **2**, the integration of the data using an orthorhombic unit cell yielded a total of 14446 reflections to a maximum θ angle of 26.41º (0.80 Å resolution), of which 2606 were independent (average redundancy 5.542, completeness = 99.4%), (Rint = 1.76%, Rsig = 2.73%) and 2582 (99.04%) were greater than $2\sigma(F^2)$. The calculated minimum and maximum transmission coefficients (based on crystal size) were 0.6994 and 0.7454. For compound **3**, the integration of the data using a monoclinic unit cell yielded a total of 122456 reflections to a maximum θ angle of 30.57º (0.70 Å resolution), of which 8875 were independent (average redundancy 13.794, completeness = 99.8%), (Rint = 3.71%, Rsig = 1.72%) and 7552 (85.06%) were greater than $2\sigma(F^2)$. The calculated minimum and maximum transmission coefficients (based on crystal size) were 0.7012 and 0.7461. For compound **4**, the integration of the data using a monoclinic unit cell yielded a total of 49555 reflections to a maxim θ angle of 30.55º (0.70 Å resolution), of which 7221 were independent (average redundancy 6.862, completeness = 99.8%), (Rint = 3.05%, Rsig = 2.23%) and 6435 (89.10%) were greater than $2\sigma(F^2)$. The calculated minimum and maximum transmission coefficients (based on crystal size) were 0.6756 and 0.7461.

The structures were solved using the Bruker SHELXTL Software, package and refined using SHELX [3]. For compound **1b**, the final anisotropic full-matrix least-squares refinement on F^2 with 304 variables converged at R1 = 3.89%, for the observed data and wR2 = 10.95% for all data. For compound **2**, the final anisotropic full-matrix least-squares refinement on F^2 with 204 variables converged at R1 = 1.60%, for the observed data and wR2 = 6.19% for all data. For compound **3**, the final anisotropic full-matrix least-squares refinement on F^2 with 417 variables converged at R1 = 4.00%, for the observed data and wR2 = 12.18% for all data. For compound **4**, the final anisotropic full-matrix least-squares refinement on F^2 with 337 variables converged at R1 = 3.27%, for the observed data and wR2 = 9.17% for all data.

For compounds **1-4**, the final cell constants and volume were based upon the refinement of the XYZ-centroids of reflections above 20 σ(I). Data were corrected for absorption effects using the multi-scan method (SADABS). Crystal data and relevant details of structure refinement for compounds **1-4** are reported in Tables S1-S2. Selected bond distances and angles are included in Tables S3-S4. Complete information about the crystal structure and molecular geometry are available in CIF format as Supporting Information. CCDC 1578832 (**1**), 1578831 (**2**), 1578834 (**3**) and 1578833 (**4**) contain the supplementary data of this paper. Molecular graphics were generated with the Mercury 3.6 software [4]. Color codes for all molecular graphics were the following: green (Zn), light blue (N), red (O), gray (C), white (H).

References

[1] (a) G. B. Deacon, R. J. Phillips, Coord. Chem. Rev. 33 (1980) 227-250; (b) K. Nakamoto, Infrared and Raman Spectra of Inorganic and Coordination Compounds. Applications in Coordination Organometallic and Bioinorganic Chemistry, 6th ed. New York, USA, 2009.

[2] (a) D. H. Williams, I. Fleming, Spectroscopic Methods in Organic Chemistry, McGrawHill, London UK, 1995; (b) E. Pretch, T. Clerc, J. Seibl, W. Simon, Tables of Determination of Organic Compounds.^{13}C NMR, ^{1}H NMR, IR, MS, UV/Vis, Chemical Laboratory Practice, Springer, Berlin, Germany, 1989.

[3] G. M. Sheldrick, Acta Cryst. C71 (2015) 3-8.

[4] (a) C. F. Macrae, P. R. Edgington, P. McCabe, E. Pidcock, G. Shields, R. Taylor, M. Towler, J. van de Streek, J. Appl. Crystallogr. 39 (2006) 453-457; (b) C. F. Macrae, I. J. Bruno, J. A. Chisholm, P. R. Edgington, P. McCabe, E. Pidcock, I. Rodriguez-Monge, R. Taylor, M. Towler, J. van de Streek, P. A. Wood, J. Appl. Crystallogr. 41(2008) 466-470.

Table S1. Crystallographic data for compound **1b.**

	1b
Empirical formula	$C_{14}H_{24}O_{15}Zn$
Formula weigh	497.70
T (K)	100(2)
Wavelength (Å)	0.71073
System, space group	Triclinic, P(-1)
Unit cell dimensions	
a (Å)	7.5115(3)
b (Å)	7.9462 (3)
c (Å)	16.1492(6)
α (º)	89.24682)
β (º)	82.283(2)
γ (º)	80.108(2)
V (Å^3)	940.93(6)
Z	2
*D*calc (g cm^3)	1.750
μ (mm^{-1})	1.387
F(000)	516
Crystal size (mm^3)	0.265x0.053x0.041
hkl ranges	-9≤h≤9 -10≤k≤10 -20≤l≤20
2θ range (º)	2.546 to 27.154
Reflections collected/ unique/[Rint]	22880/4174/[Rint] = 0.0321
Completeness to θ = 25.240	99.9%
Absorption Correction	Semi-empirical
Max. and min. transmis.	0.7455 and 0.6583
Refinement method	Full matrix least-squares on F^2
Data/restrains/parameters	4174/12/310
Goodness of fit (GOF) on F^2	1.051
Final *R* indices [$I>2\sigma(I)$]	R1 = 0.0375, wR2 = 0.0982
R indices (all data)	R1 = 0.0452 wR2 = 0.1038
Extinction coefficient	n/a
Largest. Diff. peak and hole (e Å^{-3})	2.076 and -0.579

Table S2. Crystallographic data for compounds **2-4**

	2	**3**	**4**
Empirical formula	$C_{26}H_{26}N_4O_{12}Zn$	$C_{28}H_{30}N_2O_{13}$	$C_{22}H_{24}N_4O_9Zn$
Formula weigh	651.88	667.91	553.82
T (K)	100(2)	100(2)	100(2)
Wavelength (Å)	0.71073	0.71073	0.71073
System, space group	Orthorhombic, Fdd2	Monoclinic, $P2_1/c$	Triniclic, P(-1)
Unit cell dimensions			
a (Å)	12.1575(5)	14.0101(7)	9.7497(7)
b (Å)	49.441(2)	15.5438(8)	10.0309(7)
c (Å)	8.6709(4)	13.3865(6)	12.7443(9)
α (º)	90	90	107.23(2)
β (º)	90	95.502(2)	96.043(2)
γ (º)	90	90	91.463(2)
V (Å^3)	5209.4(4)	2901.8(2)	1181.70(15)
Z	8	4	2
*D*calc (g cm^3)	1.662	1.529	1.556
μ (mm^{-1})	1.020	0.918	1.100
F(000)	2688	1384	572
Crystal size (mm^3)	0.566x0.236x0.232	0.524x0.217x0.092	0.274x0.144x0.069
hkl ranges	-15≤h≤15 -61≤k≤61 -10≤l≤10	-20≤h≤20 -22≤k≤22 -19≤l≤17	-13≤h≤13 -14≤k≤14 -18≤l≤18
2θ range (º)	2.915 to 26.407	2.400 to 30.568	2.129 to 30.554
Reflections collected/ unique/[Rint]	14446/2606/[Rint] = 0.0176	122456/8875/ [Rint] = 0.0371	49555/7221/[Rint] = 0.0305
Completeness to θ = 25.240	99.2%	99.8%	99.7
Absorption Correction	Semi-empirical	Semi-empirical	Semi-empirical
Max. and min. transmis.	0.7454 and 0.6994	0.7461and 0.7012	0.7461 and 0.6756
Refinement method	Full matrix least-squares on F^2	Full matrix least-squares on F^2	Full matrix least-squares on F^2
Data/restrains/parameters	2606/4/204	8875/3/417	7221/2/337
Goodness of fit (GOF) on F^2	1.074	1.052	1.055
Final *R* indices [$I>2\sigma(I)$]	R1 = 0.0158, wR2 = 0.0419	R1 = 0.0372, wR2 = 0.0969	R1 = 0.0326, wR2 = 0.0724
R indices (all data)	R1 = 0.0160 wR2 = 0.0621	R1 = 0.0470 wR2 = 0.1034	R1 = 0.0397 wR2 = 0.0753
Extinction coefficient	n/a	0.0041(6)	n/a
Largest. Diff. peak and hole (e Å^{-3})	0.188 and -0.289	0.676 and -0.699	0.898 and -0.627

Table S3. Selected bond lengths (Å) and bond angles (º) for compound **1b**

Bond length (Å)			
Zn(1)-O(1)	2.0209(15)	Zn(2)-O(2)	2.0350(15)
Zn(1)-O(9)	2.0728(17)	Zn(2)-O(11)	2.0365(18)
Zn(1)-O(10)	2.2581(17)	Zn(2)-O(10)	2.2495(17)
Bond angles (º)			
O(1)#1-Zn(1)-O(1)	180	O(2)#2-Zn(2)-O(2)	180
O(1)-Zn(1)-O(9)	91.25(7)	O(2)-Zn(2)-O(11)#2	91.62(7)
O(1)-Zn(1)-O(9)	88.75(7)	O(2)-Zn(2)-O(11)	88.38(7)
O(9)#1-Zn(1)-O(9)	180	O(11)#2-Zn(2)-O(11)	180
O(1)#1-Zn(1)-O(10)	88.06(6)	O(2)#2-Zn(2)-O(10)	89.49(6)
O(1)-Zn(1)-O(10)	92.13(7)	O(2)-Zn(2)-O(10)	90.51(6)
O(9)#1-Zn(1)-O(10)	88.35(7)	O(11)-Zn(2)-O(10)	88.40(7)
O(9)-Zn(1)-O(10)	91.94(6)	O(11)-Zn(2)-O(10)#2	91.60(7)
O(10)-Zn(1)-O(10)#1	180	O(10)-Zn(2)-O(10)#2	180

#1 –x+1, -y+2,-z; #2 –x+1, -y+1, -z

Table S4. Selected bond lengths (Å) and bond angles (º) for compounds **2-4**

2			
Bond length (Å)			
Zn(1)-O(1)	1.9454(7)	Zn(1)-N(1)	2.035(2)
Bond angles (º)			
O(1)-Zn(1)-O(1)#1	106.14(10)	O(1)-Zn(1)-N(1)#1	123.72(8)
O(1)-Zn(1)-N(1)	97.44(8)	N(1)-Zn(1)-N(1)#1	110.53(12)
3			
Bond length (Å)			
Zn(1)-O(5)	1.9757(12)	Zn(1)-N(2)	2.0283(5)
Zn(1)-O(1)	1.9831(12)	Zn(1)-N(1)	2.0643(16)
Bond angles (º)			
O(5)-Zn(1)-O(1)	103.20(5)	O(5)-Zn(1)-N(1)	95.94(6)
O(5)-Zn(1)-N(2)	117.76(6)	O(1)-Zn(1)-N(1)	117.85(6)
O(1)-Zn(1)-N(2)	115.62(6)	N(2)-Zn(1)-N(1)	105.37(6)
4			
Bond length (Å)			
Zn(1)-O(5)	1.9874(12)	Zn(1)-N(1)	2.0148(14)
Zn(1)-O(2)	2.1803(11)	Zn(1)-N(3)	2.0370(14)
Zn(1)-O(1)	2.1971(12)		
Bond angles (º)			
O(5)-Zn(1)-N(1)	110.07(5)	N(3)-Zn(1)-O(2)	85.75(5)
O(5)-Zn(1)-N(3)	116.30(5)	O(5)-Zn(1)-O(1)	112.52(5)
N(1)-Zn(1)-N(3)	100.06(6)	N(1)-Zn(1)-O(1)	92.08(5)
O(5)-Zn(1)-O(2)	93.61(5)	N(3)-Zn(1)-O(1)	121.14(5)

2: #-x+1, -y+1, z

Table S5. Distances [Å] and angles [deg.] related to hydrogen bonding interaction in complexes **1b-4.**

1b	[Å]	[Å]	[deg]	
D-H···A	H···A	D···A	> D-H···A	Symmetry code
O11-H11A···O5	1.90	2.720	171	1+x,1+y,z
O3-H3A···O8	1.86	2.692	172	x,y,z
O9-H9B···O6	1.96	2.757	160	1-x,2-y,1-z
O9-H9A···O6	1.90	2.733	176	1-x,3-y,-z
O11-H11···O5	1.97	2.747	167	1-x,2-y,-z
O10-H2B···O3W	1.84	2.705	176	1-x,2-y,-z
O10-H1A···O4W	1.94	2.733	172	-x,2-y,1-z
O4W-H4WA···O5	1.95	2.729	171	1-x,2-y,1-z
O3W-H3W···O6	1.96	2.766	166	1-x,2-y,1-z
2				
N2-H2NA···O5	2.22	3.006	149	¼+x,¼-y,¼+z
N2-H2NB···O3	2.13	2.932	151	½+x,y,3/2+z
O1W-H1WA···O4	1.96	2.774	168	¼+x,¼-y,¼+z
O3-H3O···O2	1.77	2.598	166	-½-x,-y,-½+z
O1W-H1WB···O5	1.95	2.774	169	-¼+x,¼-y,¼+z
O4-H4O···O1W	1.80	2.611	163	½+x,y,3/2+z
3				
O3W-H3AW···O2W	1.94	2.752	167	x,y,z
O3W-H3BW···O7	1.95	2.736	161	1-x,1-y,1-z
O3-H3O···O3W	1.83	2.618	157	-x,½+y,½+z
O4-H4···O6	1.81	2.559	171	x,3/2-y,-½+z
O7-H7O···O1W	1.76	2.591	172	x,1+y,z
O8-H8O···O2	2.26	2.695	113	1-x,1-y,1-z
4				
O1W-H1W···O1	2.06	2.852	172	1-x,1-y,1-z
O1W-H2W···O7	2.02	2.799	171	x,y,z
O3-H3O···O6	1.83	2.671	179	1-x,1-y,1-z
N4-H4N···O2	2.26	2.847	124	1-x,1-y,1-z
O4-H4O-O1W	1.85	2.654	171	1+x,1+y,z
O7-H7O···O3	2.03	2.809	179	x,-1+y,-1+z
O8-H8O···O4	2.01	2.798	156	1-x,2-y,1-z

Additional Figures

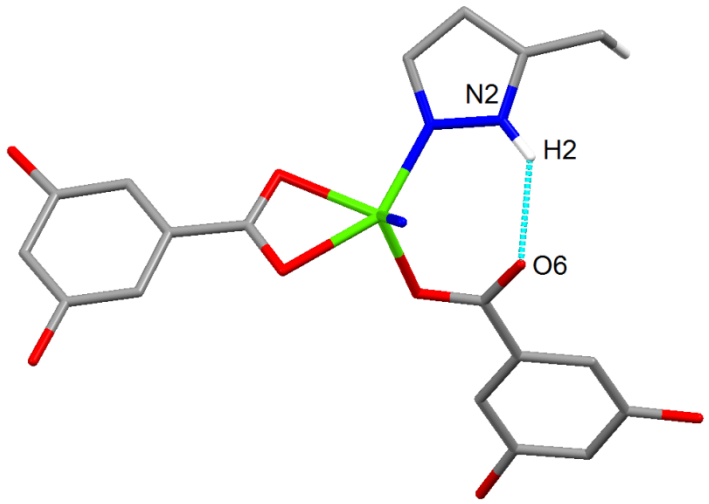

Figure S1. Detail of the intramolecular interaction N-H···O in [Zn(μ-3,5-DHB)$_2$(3-Mepz)$_2$]·H$_2$O (**4**). Only one N atom of the pyrazole ligand not involved in this intramolecular bond is depicted for clarity

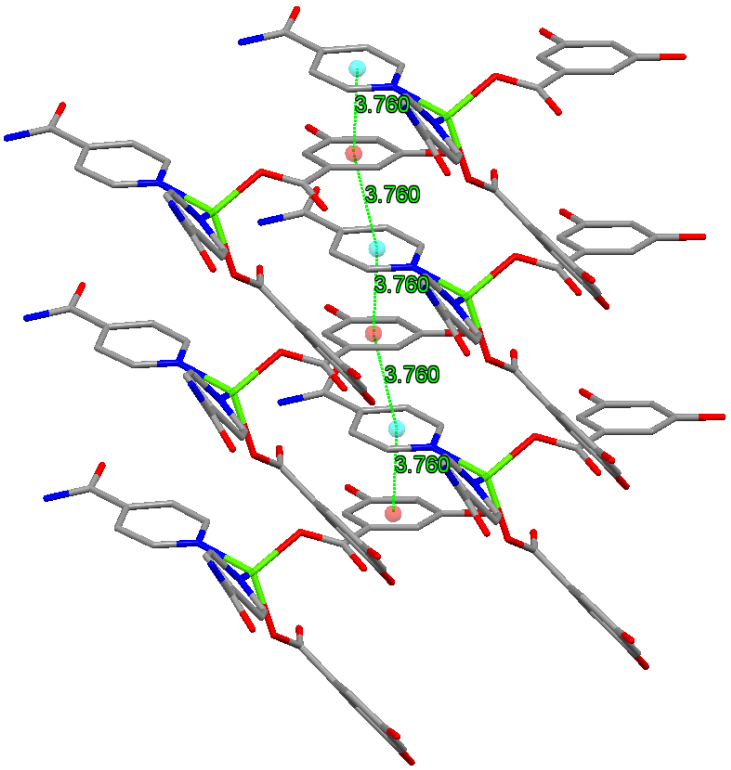

Figure S2. Detail of the π-stacking interactions in [Zn(3,5-DHB)$_2$(Isna)$_2$]·2H$_2$O (**2**).

.

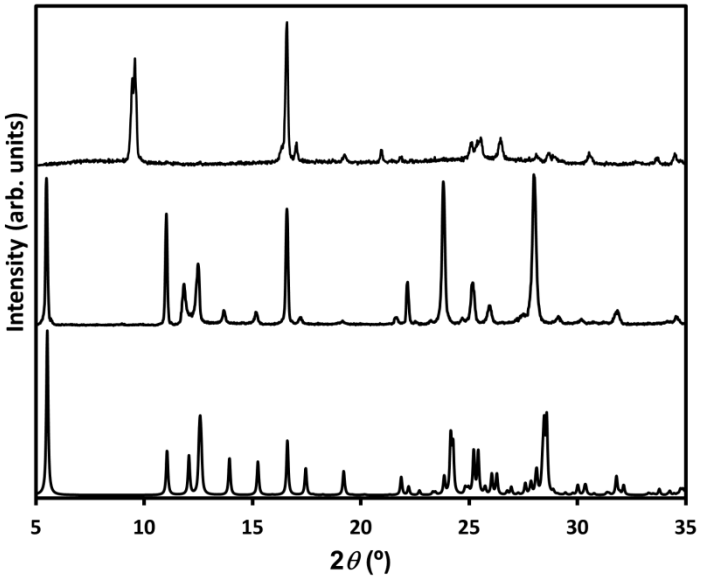

Figure S3. X-ray diffractograms of [Zn(μ-3,5-DHB)$_2$(H_2O)$_2$] (**1a**) (up) and {[Zn(μ-3,5-DHB)(μ-OH_2)(H_2O)$_2$]$_n$·(3,5-DHB)$_n$·(4H_2O)$_n$}**(1b) (**middle) measured at room temperature. Calculated pattern from resolved crystal structure (down) as a reference, from single crystal XRD measured at 100 K**.**

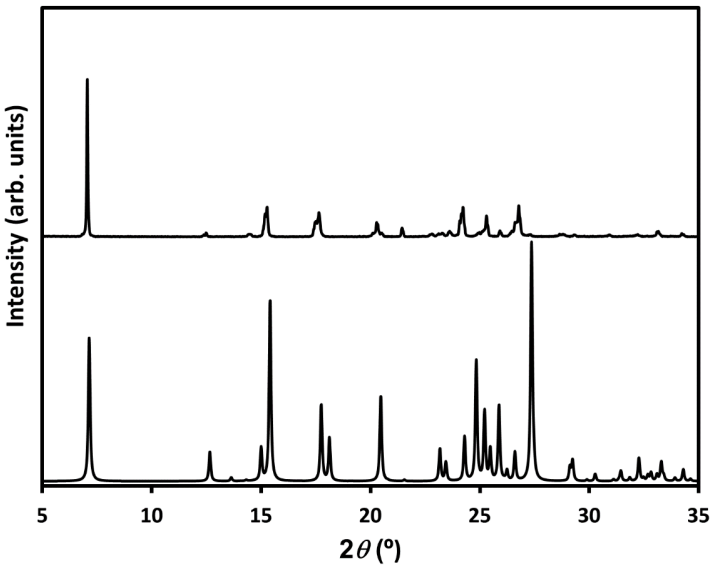

Figure S4. X-ray diffractograms of {[Zn(3,5-DHB)$_2$(isna)$_2$]·2H_2O} **(2)** (up) measured at room temperature. Calculated pattern from resolved crystal (down) as a reference, from single crystal XRD measured at 100 K.

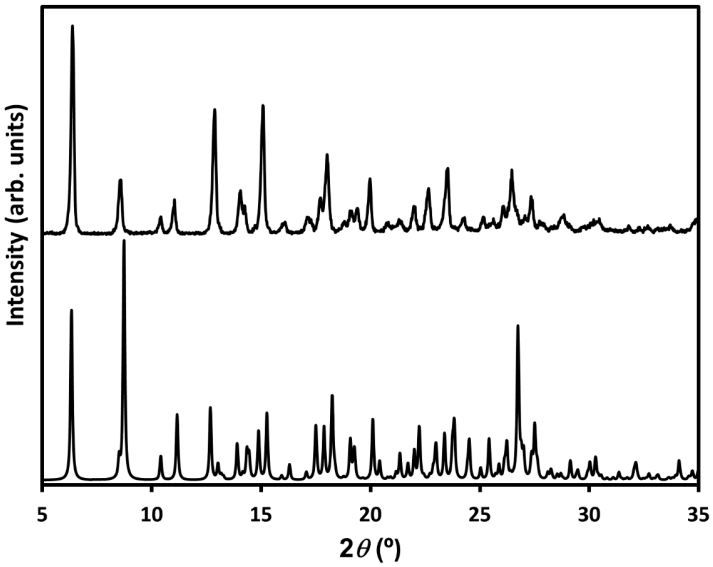

Figure S5. X-ray diffractograms of {[Zn(3,5-DHB)$_2$(4-Acpy)$_2$]·3H$_2$O} **(3)** (up) measured at room temperature. Calculated pattern from resolved crystal structure (down) as a reference, from single crystal XRD measured at 100 K.

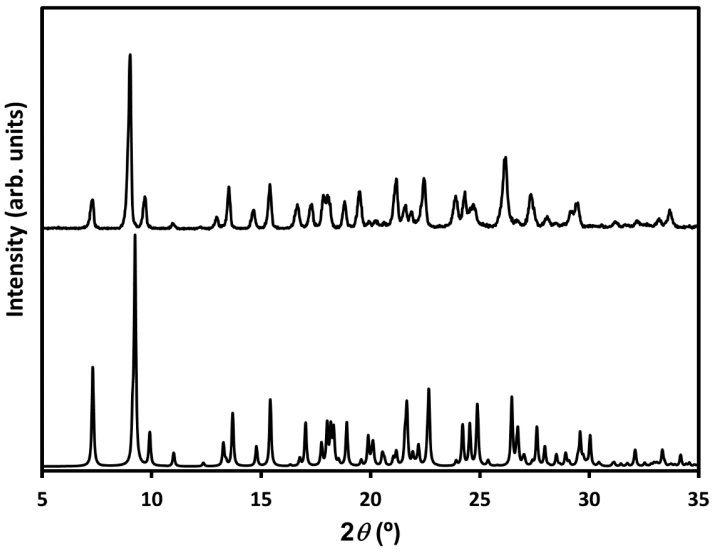

Figure S6. X-ray diffractograms of {[Zn(3,5-DHB)$_2$(3-Mepz)$_2$]·H$_2$O} **(4)** (up) measured at room temperature. Calculated pattern from resolved crystal (down) as a reference, from single crystal XRD measured at 100 K.